



ARTICLE

Estimation of a Line Heat Source Using an Adjoint Free Gradient Based Inverse Analysis

Farzad Mohebbi*

Department of Mechanical Engineering, The University of Canterbury, Christchurch, 8140, New Zealand

*Corresponding Author: Farzad Mohebbi. Email: farzadmohebbi@yahoo.com

Received: 12 June 2025; Accepted: 25 July 2025; Published: 31 October 2025

ABSTRACT: An inverse analysis is presented to estimate line heat source in two-dimensional steady-state and transient heat transfer problems. A constant heat source is considered in the steady-state heat transfer problem (a parameter estimation problem) and a time-varying heat source is considered in the transient heat transfer problem (a function estimation problem). Since a general irregular 2D heat conducting body is considered, a body-fitted grid generation is used to mesh the domain. Then governing equations and associated boundary and initial conditions are transformed from the physical domain to the computational domain and finite difference method is used to solve the governing equations to obtain the temperature distribution in the body. Using an efficient, accurate, and very easy to implement sensitivity analysis incorporated in a gradient based minimization method (here, steepest descent method), the unknown heat source is estimated accurately. In the function estimation part, it is assumed that there is no prior information on the functional form of the heat source and the estimation process can be performed with a reasonable initial guess for the heat source. The main advantage of the proposed inverse analysis is that the sensitivity matrix (and hence, the objective function gradient with respect to the unknown variables) can be computed during the direct heat transfer solution through new yet simple explicit expressions with no need to solve extra equations such as the sensitivity and adjoint problems and impose additional computational costs comparable to the direct problem solution ones. Some test cases are presented to investigate the accuracy, efficiency, and effect of measurement error on the estimated parameter and function for the line heat source.

KEYWORDS: Inverse heat conduction; finite difference method; function estimation; gradient based minimization; line heat source

1 Introduction

Due to the ever increasing power and capacity of computers as well as the development of different numerical methods over the past decades, inverse heat transfer problems have been subject of intensive research. These problems are mathematically classified as ill-posed as their solutions are unstable and very sensitive to the errors in the measurements used in the analysis [1]. Among the numerical methods to overcome the instabilities present in these problems are iterative regularization techniques which are based on the improving the inverse problem solution sequentially through an iterative minimization method such as steepest descent and conjugate gradient method and then stopping the inverse analysis process when a stable solution is obtained [2]. The determination of the functional form of an unknown quantity (such as heat flux, heat transfer coefficient, and heat source) in the inverse heat transfer problems is a difficult task as the problem falls into the category of function estimation approach [3,4]. In the inverse



heat transfer problems with no a priori information on the functional form, the function estimation approach is usually concerned with the solution of two additional problems, namely, sensitivity and adjoint problems. The solution of these two problems requires additional mathematical manipulation and imposes the computational cost comparable to direct problem solution one on the inverse analysis [1].

The estimation of the heat source using an inverse analysis has received considerable attention over past decades [5–7]. It has many practical applications in various engineering fields such as welding processes [8,9]. In [10], the unknown functional form of a timewise varying strength of a line heat source is estimated using the conjugate gradient method. The heat source is placed at the specific location in a regular 2D physical domain with insulated boundaries. In [11], the time-varying strength of a heat source in a two-dimensional heat conduction problem is estimated using a method based on the Karhunen-Loeve Galerkin procedure and the conjugate gradient method. In [12], based on the finite element method and the conjugate gradient, both the location and the time-varying strength of point heat sources within a body are estimated from temperature boundary measurements. In [13], a genetic algorithm is used to estimate plane heat source in an one-dimensional domain with insulated boundaries. In [8], a multiple model adaptive inverse method is used to estimate a moving heat source. In [14], a meshless numerical scheme is presented for recovering the time-dependent heat source in general three-dimensional heat conduction problems. The second-order Crank–Nicolson scheme is employed for discretization in time-domain. In [15], a meshless numerical scheme is presented for solving the inverse heat source problem using the fundamental solution of the heat equation as a basis function. A regularized solution is obtained by employing the Tikhonov regularization method. In [16], the inverse problem of determination of the time-dependent heat source under a non-classical dynamic boundary condition has been considered. The numerical solution of the inverse problem includes the boundary element method combined with the second-order Tikhonov regularization. In [17], the time-varying heat source in one-dimensional heat conduction is estimated using conjugate gradient method combined with the adjoint problem for three types of source variations including constant, linearly increasing, and linearly decreasing ones. In [18], unknown parameters of a time-varying plane heat source in a one-dimensional inverse heat conduction problem are estimated using Repulsive Particle Swarm Optimization (RPSO) method. Then the results are compared with those of the Levenberg-Marquardt Method, a widely used minimization method in the inverse heat conduction problems. In [19], unknown heat source strength in three-dimensional inverse heat conduction problems is studied. The direct problem is solved by applying the Green's function method. The Tikhonov and truncated singular value decomposition regularization methods are developed to identify the unknown source strength.

In the literature, however, there are still some limitations on the methods used to identify the variables involved in the inverse heat transfer problems such as the heat source. For example, most of the heated body shapes considered are regular (rectangular or circular) or most of the boundary conditions considered include a constant temperature (Dirichlet boundary condition) or insulated case. Thus a methodology considering a general irregular 2D domain with a variety of boundary conditions is required.

The numerical method proposed in this study deals with 2D irregular physical domains and a variety of boundary conditions. It can also be extended to 3D problems and other heat source types such as point and plane heat sources. In this method, the irregular physical domain and all associated boundary conditions are transformed from the physical domain to the computational one so that the finite difference method can be used to solve the heat conduction equation for the irregular body shapes. A very easy to implement sensitivity analysis is proposed based on chain rule and direct differentiation which enables us to calculate all elements of the sensitivity matrix during the direct problem solution (at each iteration) without dealing with the sensitivity and adjoint problems to calculate the gradient of defined least squares objective function. After computation of the sensitivity matrix, the gradient of the objective function and search step size can

be computed easily through explicit expressions. The steepest descent method, an iterative gradient based minimization method, is used to minimize the objective function. In this study, both the steady-state (for a constant heat source, a parameter estimation problem) and transient (for a time-varying heat source, a function estimation problem) heat conduction problems are considered. In the function estimation part, it is assumed that there is no prior information on the functional form of the heat source and the estimation process can be performed with a reasonable initial guess for the heat source.

2 Governing Equation

2.1 Transient Heat Conduction

Consider an irregular heat-conducting body of thermal conductivity k_T , density ρ , and specific heat c which is initially at the temperature T_0 (Fig. 1). At time $t > 0$, a heat flux \dot{q} is applied at boundary surface Γ_1 , a convective heat transfer is applied at the boundaries Γ_i , $i = 2, 3, 4$ with corresponding heat transfer coefficients h_i , $i = 2, 3, 4$ and surrounding temperatures T_{∞_i} , $i = 2, 3, 4$, and heat is generated continuously over time at the point L_{x^\dagger, y^\dagger} with a line heat source of strength $g_L(t)$ ($\frac{W}{m}$). The transient heat transfer equation can be expressed as

$$k_T \left(\frac{\partial^2 T(x, y, t)}{\partial x^2} + \frac{\partial^2 T(x, y, t)}{\partial y^2} \right) + g(x, y, t) = \rho c \frac{\partial T(x, y, t)}{\partial t} \quad (1)$$

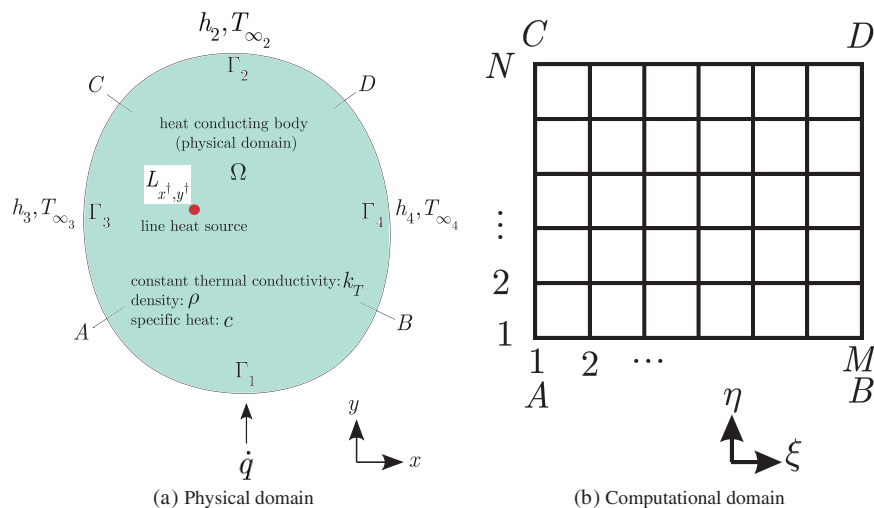


Figure 1: Irregular heat-conducting body (physical domain) subjected to a heat flux \dot{q} on surface Γ_1 , a line heat source at point L_{x^\dagger, y^\dagger} , and convective heat transfer on surfaces Γ_i , $i = 2, 3, 4$ (a) and the corresponding computational domain (b)

The line heat source of time-varying strength $g_L(t)$ ($\frac{W}{m}$) is related to the volumetric source $g(x, y, t)$ ($\frac{W}{m^3}$) by the delta function notation as [20]

$$g(x, y, t) = g_L(t) \delta(x - x^\dagger) \delta(y - y^\dagger) \quad (2)$$

where t is the time and $\delta(-)$ represents the Dirac delta function and approximates the source in the domain and is defined by [11]

$$\delta_n(x - x^\dagger) \approx \frac{n}{2 \cosh^2(n(x - x^\dagger))}, \delta_n(y - y^\dagger) \approx \frac{n}{2 \cosh^2(n(y - y^\dagger))} \quad (3)$$

where (x^\dagger, y^\dagger) is the location of time-varying line heat source. The function δ_n becomes the Dirac delta function as n approaches infinity. In this study, we take $n = 80$. Each of the delta functions in Eq. (2) has the units of $(\frac{1}{m})$. Thus the unit for the volumetric source $g(x, y, t)$ is as $(\frac{W}{m})(\frac{1}{m})(\frac{1}{m}) = (\frac{W}{m^3})$. Eq. (1) can be expressed as

$$k_T \left(\frac{\partial^2 T(x, y, t)}{\partial x^2} + \frac{\partial^2 T(x, y, t)}{\partial y^2} \right) + g_L(t) \delta_n(x - x^\dagger) \delta_n(y - y^\dagger) = \rho c \frac{\partial T(x, y, t)}{\partial t}$$

$$\text{in the physical domain } \Omega(x, y), t > 0 \quad (4)$$

with the boundary and initial conditions

$$\frac{\partial T(x, y, t)}{\partial n_1} = \frac{\dot{q}}{k_T} \text{ on boundary surface } \Gamma_1(x, y) \quad (5)$$

$$\frac{\partial T(x, y, t)}{\partial n_i} = -\frac{h_i}{k_T} (T_{\Gamma_i}(x, y, t) - T_{\infty_i}) \text{ on boundary surface } \Gamma_i(x, y), i = 2, 3, 4 \quad (6)$$

$$T(x, y, 0) = T_0(x, y) \text{ in physical domain } \Omega(x, y) \quad (7)$$

First the heat-conducting body is mapped from the irregular x, y physical domain (Fig. 1a) to the regular ξ, η computational domain (Fig. 1b). The elliptic grid generation method is used to mesh the irregular physical domain. Then by transforming the heat conduction equation and the boundary and initial conditions from the (x, y, t) to the (ξ, η, t) variables, we obtain [21]

$$k_T \left(\frac{\alpha \frac{\partial^2 T(\xi, \eta, t)}{\partial \xi^2} - 2\beta \frac{\partial^2 T(\xi, \eta, t)}{\partial \xi \partial \eta} + \gamma \frac{\partial^2 T(\xi, \eta, t)}{\partial \eta^2}}{J^2} + (\nabla^2 \xi) \frac{\partial T(\xi, \eta, t)}{\partial \xi} + (\nabla^2 \eta) \frac{\partial T(\xi, \eta, t)}{\partial \eta} \right) + g_L(t) \frac{n^2}{4 \cosh^2(n(x - x^\dagger)) \cosh^2(n(y - y^\dagger))} = \rho c \frac{\partial T(\xi, \eta, t)}{\partial t} \quad (8)$$

where $\nabla^2 \xi = P(\xi, \eta)$ and $\nabla^2 \eta = Q(\xi, \eta)$ are grid control functions. By considering $P(\xi, \eta) = Q(\xi, \eta) = 0$ to obtain a smooth grid over the physical domain, we obtain

$$k_T \left(\frac{\alpha \frac{\partial^2 T(\xi, \eta, t)}{\partial \xi^2} - 2\beta \frac{\partial^2 T(\xi, \eta, t)}{\partial \xi \partial \eta} + \gamma \frac{\partial^2 T(\xi, \eta, t)}{\partial \eta^2}}{J^2} \right) + \frac{n^2 g_L(t)}{4 \cosh^2(n(x - x^\dagger)) \cosh^2(n(y - y^\dagger))} = \rho c \frac{\partial T(\xi, \eta, t)}{\partial t} \text{ in } 1 < \xi < M, 1 < \eta < N, \text{ for } t > 0 \quad (9)$$

where

$$\alpha = x_\eta^2 + y_\eta^2$$

$$\beta = x_\xi x_\eta + y_\xi y_\eta$$

$$\gamma = x_\xi^2 + y_\xi^2$$

$$J = x_\xi y_\eta - x_\eta y_\xi \text{ (Jacobian of transformation)} \quad (10)$$

The boundary and initial conditions can be transformed as

$$\left(\frac{-1}{J\sqrt{\gamma}} \left(\gamma \frac{\partial T(\xi, \eta, t)}{\partial \eta} - \beta \frac{\partial T(\xi, \eta, t)}{\partial \xi} \right) \right)_{\Gamma_1} = \frac{\dot{q}}{k_T} \text{ at } 1 < \xi < M, \eta = 1, \text{ for } t > 0 \quad (11)$$

$$\left(\frac{1}{J\sqrt{\gamma}} \left(\gamma \frac{\partial T(\xi, \eta, t)}{\partial \eta} - \beta \frac{\partial T(\xi, \eta, t)}{\partial \xi} \right) \right)_{\Gamma_2} = -\frac{h_2}{k_T} (T(\xi, \eta, t) - T_{\infty_2}) \text{ at } 1 < \xi < M, \eta = N, \text{ for } t > 0 \quad (12)$$

$$\left(\frac{-1}{J\sqrt{\alpha}} \left(\alpha \frac{\partial T(\xi, \eta, t)}{\partial \xi} - \beta \frac{\partial T(\xi, \eta, t)}{\partial \eta} \right) \right)_{\Gamma_3} = -\frac{h_3}{k_T} (T(\xi, \eta, t) - T_{\infty_3}) \text{ at } 1 < \eta < N, \xi = 1, \text{ for } t > 0 \quad (13)$$

$$\left(\frac{1}{J\sqrt{\alpha}} \left(\alpha \frac{\partial T(\xi, \eta, t)}{\partial \xi} - \beta \frac{\partial T(\xi, \eta, t)}{\partial \eta} \right) \right)_{\Gamma_4} = -\frac{h_4}{k_T} (T(\xi, \eta, t) - T_{\infty_4}) \text{ at } 1 < \eta < N, \xi = M, \text{ for } t > 0 \quad (14)$$

$$T(\xi, \eta, 0) = T_0^*(\xi, \eta) \text{ in } 1 < \xi < M, 1 < \eta < N, \text{ for } t = 0 \quad (15)$$

Using the finite difference method to discretize the derivatives in the resulting equations in the computational domain, we obtain (assuming $\Delta\xi = \Delta\eta = 1$)

$$f_\xi = \frac{1}{2} (f_{i+1,j} - f_{i-1,j})$$

$$f_\eta = \frac{1}{2} (f_{i,j+1} - f_{i,j-1})$$

$$f_{\xi\xi} = f_{i+1,j} - 2f_{i,j} + f_{i-1,j}$$

$$f_{\eta\eta} = f_{i,j+1} - 2f_{i,j} + f_{i,j-1}$$

$$f_{\xi\eta} = \frac{1}{4} (f_{i+1,j+1} - f_{i-1,j+1} - f_{i+1,j-1} + f_{i-1,j-1}) \quad (16)$$

where $f \equiv x, y, T$. To discretize the boundary condition equations, one may use one-sided forward and one-sided backward expressions. Using the forward-time-central-space (FTCS) scheme (an explicit method), we obtain [21]

$$\frac{k_T}{J^2} \left(\alpha (T_{i+1,j}^n - 2T_{i,j}^n + T_{i-1,j}^n) - 2\beta \frac{(T_{i+1,j+1}^n - T_{i-1,j+1}^n - T_{i+1,j-1}^n + T_{i-1,j-1}^n)}{4} + \gamma (T_{i,j+1}^n - 2T_{i,j}^n + T_{i,j-1}^n) \right) +$$

$$\frac{n^2 g_L(t)}{4 \cosh^2(n(x-x^\dagger)) \cosh^2(n(y-y^\dagger))} = \rho c \frac{T_{i,j}^{n+1} - T_{i,j}^n}{\Delta t}, i = 2, \dots, M-1, j = 2, \dots, N-1, \text{ for } t > 0 \quad (17)$$

where Δt is the time step. The time-marching method is used to calculate $T_{i,j}^{n+1}$, the nodal temperatures at the time level $n+1$, by knowing the nodal temperatures at the previous time level n , $T_{i,j}^n$. Thus we obtain the following explicit expression for the transient heat conduction equation

$$T_{i,j}^{n+1} = T_{i,j}^n + \frac{\Delta t}{\rho c} \frac{n^2 g_L(t)}{4 \cosh^2(n(x-x^\dagger)) \cosh^2(n(y-y^\dagger))} + \frac{k_T \Delta t}{\rho c J^2} \left(\alpha (T_{i+1,j}^n - 2T_{i,j}^n + T_{i-1,j}^n) - 2\beta \frac{(T_{i+1,j+1}^n - T_{i-1,j+1}^n - T_{i+1,j-1}^n + T_{i-1,j-1}^n)}{4} + \gamma (T_{i,j+1}^n - 2T_{i,j}^n + T_{i,j-1}^n) \right) \quad (18)$$

2.2 Steady-State Heat Conduction

With the same explanations for transforming the transient heat condition equation, we can obtain the transformed relations for the steady-state heat conduction equation. Then by substituting the finite difference expressions given in Eq. (16) into the obtained steady-state equation, and then solving for $T_{i,j}$ we obtain ($i = 2, \dots, M-1; j = 2, \dots, N-1$)

$$T_{i,j} = \frac{1}{2(\alpha + \gamma)} \left(\alpha T_{i+1,j} + \alpha T_{i-1,j} - 2\beta T_{\xi\eta} + \gamma T_{i,j+1} + \gamma T_{i,j-1} + \frac{J^2 n^2 g_L}{k_T 4 \cosh^2(n(x-x^\dagger)) \cosh^2(n(y-y^\dagger))} \right) \quad (19)$$

where from Eq. (16), $T_{\xi\eta} = 1/4 (T_{i+1,j+1} - T_{i-1,j+1} - T_{i+1,j-1} + T_{i-1,j-1})$. An iterative method such as Gauss-Seidel or Successive Over-Relaxation (SOR) method can be used to solve the steady-state heat conduction equation, Eq. (19), and the boundary conditions.

3 Inverse Analysis

3.1 Objective Function for Transient Heat Conduction

As in this study, two separate inverse heat transfer problems are considered (the transient and steady-state cases), the objective function expressions are defined separately for each case. For the transient heat transfer problem, the inverse analysis is concerned with the estimation of the time-varying line heat source strength $g_L(t)$ applied at the time t_i ($i = 1, \dots, r$ where r is the number of time steps) and the place (x^\dagger, y^\dagger) using the transient temperature measurements of a single sensor S placed at the point (Si, Sj) inside the body. In the transient inverse analysis, the aim is to minimize the difference between the estimated temperatures at the sensor place, $T_e(Si, Sj, t_i)$, which is obtained from the solution of the direct transient heat conduction equation using the estimated line heat source strength $g_L(t_i)$, and the measured temperatures $T_m(Si, Sj, t_i)$ over the time domain $0 < t < t_r$ as much as possible. Thus the objective function can be mathematically expressed as

$$\min \left\{ \mathcal{J}_{\text{gl at } (x^\dagger, y^\dagger)} := \|T_e(Si, Sj, t) - T_m(Si, Sj, t)\|^2 : \text{Eq.(4) in } \Omega, \text{BCs and IC in Eqs.(5)-(7)} \right\} \quad (20)$$

where $\mathbf{g}_L = [g_L(t_1), g_L(t_2), g_L(t_3), \dots, g_L(t_r)]^T$. Therefore,

$$\mathcal{J} = \sum_{i=1}^r [T_e(S_i, S_j, t_i) - T_m(S_i, S_j, t_i)]^2 \quad (21)$$

Sensitivity Analysis for Transient Heat Conduction

In this study, a gradient based minimization method (steepest descent method) is used to minimize the objective function value for both the transient and steady-state problems. Thus the gradient of the objective function with respect to the unknown variables is required. In the transient inverse problem, the gradient of the objective function \mathcal{J} defined by Eq. (21) with respect to $g_L(t_i)$, $i = 1, \dots, r$ can be obtained by

$$\frac{\partial \mathcal{J}}{\partial g_L(t_{i'})} = 2 \sum_{i=1}^r [T_e(S_i, S_j, t_i) - T_m(S_i, S_j, t_i)] \frac{\partial T_e(S_i, S_j, t_i)}{\partial g_L(t_{i'})} \quad (22)$$

This is a function estimation problem and there is no prior information on the functional form of the unknown variable (here the line heat source strength $g_L(t)$). The function estimation problems are usually solved using the adjoint problem to obtain the gradient of the objective function. However, the adjoint method comes with mathematical complexity. In addition, the adjoint equation solution itself has a computational cost comparable to the direct solution. Here, as it will be shown, using a parameter estimation approach, the unknown functional form of the line heat source strength can be calculated efficiently and accurately without solving the additional equations. In the proposed method, the elements of the sensitivity matrix are calculated during the heat conduction equation solution using some explicit expressions. Using the chain rule, we can write [22]

$$\frac{\partial T_e(S_i, S_j, t_i)}{\partial g_L(t_{i'})} = \frac{\left(\frac{\partial T_e(S_i, S_j, t_i)}{\partial k_T} \right) \Big|_{\text{at sensor place } S}}}{\left(\frac{\partial g_L(t_{i'})}{\partial k_T} \right) \Big|_{\text{at source place } L}} \quad (23)$$

This implies that two variables at two different times t_i and $t_{i'}$ can be related using a constant variable (here the constant thermal conductivity k_T). The term $\frac{\partial T_e(S_i, S_j, t_i)}{\partial k_T}$ can be obtained by taking derivative of $T_{i,j}^{n+1}$ in Eq. (18) with respect to k_T , as follows

$$\begin{aligned} \frac{\partial T_e^{n+1}(S_i, S_j)}{\partial k_T} &= \frac{\Delta t}{\rho c J^2} \left(\alpha (T_{Si+1, Sj}^n - 2T_{Si, Sj}^n + T_{Si-1, Sj}^n) \right. \\ &\quad \left. - 2\beta \frac{1}{4} (T_{Si+1, Sj+1}^n - T_{Si-1, Sj+1}^n - T_{Si+1, Sj-1}^n + T_{Si-1, Sj-1}^n) + \gamma (T_{Si, Sj+1}^n - 2T_{Si, Sj}^n + T_{Si, Sj-1}^n) \right) \end{aligned} \quad (24)$$

In Eq. (23), $\frac{\partial g_L(t_{i'})}{\partial k_T}$ can be obtained by initially solving Eq. (9) for $g_L(t)$ and then taking the derivative of the resulting expression with respect to k_T , as follows

$$g_L(t_{i'}) = \frac{\rho c \frac{\partial T(\xi, \eta, t)}{\partial t} (4 \cosh^2(n(x - x^\dagger)) \cosh^2(n(y - y^\dagger)))}{n^2} -$$

$$\frac{k_T (4 \cosh^2 (n(x - x^\dagger)) \cosh^2 (n(y - y^\dagger)))}{J^2 n^2} \left(\alpha \frac{\partial^2 T(Li, Lj, t_{i'})}{\partial \xi^2} - 2\beta \frac{\partial^2 T(Li, Lj, t_{i'})}{\partial \xi \partial \eta} + \gamma \frac{\partial^2 T(Li, Lj, t_{i'})}{\partial \eta^2} \right) \quad (25)$$

thus

$$\frac{\partial g_L(t_{i'})}{\partial k_T} = - \frac{(4 \cosh^2 (n(x - x^\dagger)) \cosh^2 (n(y - y^\dagger))) \left(\alpha \frac{\partial^2 T(Li, Lj, t_{i'})}{\partial \xi^2} - 2\beta \frac{\partial^2 T(Li, Lj, t_{i'})}{\partial \xi \partial \eta} + \gamma \frac{\partial^2 T(Li, Lj, t_{i'})}{\partial \eta^2} \right)}{J^2 n^2} \quad (26)$$

$\frac{\partial g_L(t_{i'})}{\partial k_T}$ is calculated at the heat source place at $L(x = x^\dagger, y = y^\dagger)$ which corresponds to $L(Li, Lj)$ in the computational domain. Therefore,

$$\cosh^2(n(x - x^\dagger)) \cosh^2(n(y - y^\dagger))|_{(x=x^\dagger, y=y^\dagger)} = 1 \quad (27)$$

And Eq. (26) becomes

$$\frac{\partial g_L(t_{i'})}{\partial k_T} = - (4) \frac{\left(\alpha \frac{\partial^2 T(Li, Lj, t_{i'})}{\partial \xi^2} - 2\beta \frac{\partial^2 T(Li, Lj, t_{i'})}{\partial \xi \partial \eta} + \gamma \frac{\partial^2 T(Li, Lj, t_{i'})}{\partial \eta^2} \right)}{J^2 n^2} \quad (28)$$

Now all the sensitivity coefficients $\frac{\partial T_e(Si, Sj, t_i)}{\partial g_L(t_{i'})}$ can be calculated during the solution of the transient heat conduction equation (direct solution). The sensitivity matrix $\mathbf{J}\mathbf{a}$ can be explicitly expressed as

$$\mathbf{J}\mathbf{a}_{g_L(t)} = \begin{bmatrix} \frac{\partial T_e(Si, Sj, t_1)}{\partial g_L(t_1)} & \frac{\partial T_e(Si, Sj, t_1)}{\partial g_L(t_2)} & \frac{\partial T_e(Si, Sj, t_1)}{\partial g_L(t_3)} & \cdots & \frac{\partial T_e(Si, Sj, t_1)}{\partial g_L(t_r)} \\ \frac{\partial T_e(Si, Sj, t_2)}{\partial g_L(t_1)} & \frac{\partial T_e(Si, Sj, t_2)}{\partial g_L(t_2)} & \frac{\partial T_e(Si, Sj, t_2)}{\partial g_L(t_3)} & \cdots & \frac{\partial T_e(Si, Sj, t_2)}{\partial g_L(t_r)} \\ \frac{\partial T_e(Si, Sj, t_3)}{\partial g_L(t_1)} & \frac{\partial T_e(Si, Sj, t_3)}{\partial g_L(t_2)} & \frac{\partial T_e(Si, Sj, t_3)}{\partial g_L(t_3)} & \cdots & \frac{\partial T_e(Si, Sj, t_3)}{\partial g_L(t_r)} \\ \vdots & \vdots & \vdots & \ddots & \vdots \\ \frac{\partial T_e(Si, Sj, t_r)}{\partial g_L(t_1)} & \frac{\partial T_e(Si, Sj, t_r)}{\partial g_L(t_2)} & \frac{\partial T_e(Si, Sj, t_r)}{\partial g_L(t_3)} & \cdots & \frac{\partial T_e(Si, Sj, t_r)}{\partial g_L(t_r)} \end{bmatrix}_{r \times r} \quad (29)$$

At any time t , the current temperature distribution is independent of a future heat source component which means that the sensitivity matrix is lower-triangular. In other words, for $i' > i$ (the elements above the main diagonal of the sensitivity matrix), $\frac{\partial T_e(Si, Sj, t_i)}{\partial g_L(t_{i'})} = 0$. So, the sensitivity matrix will be as follows

$$\mathbf{J}\mathbf{a}_{g_L(t)} = \begin{bmatrix} \frac{\partial T_e(Si, Sj, t_1)}{\partial g_L(t_1)} & 0 & 0 & \dots & 0 \\ \frac{\partial T_e(Si, Sj, t_2)}{\partial g_L(t_1)} & \frac{\partial T_e(Si, Sj, t_2)}{\partial g_L(t_2)} & 0 & \dots & 0 \\ \frac{\partial T_e(Si, Sj, t_3)}{\partial g_L(t_1)} & \frac{\partial T_e(Si, Sj, t_3)}{\partial g_L(t_2)} & \frac{\partial T_e(Si, Sj, t_3)}{\partial g_L(t_3)} & \dots & 0 \\ \vdots & \vdots & \vdots & \ddots & \vdots \\ \frac{\partial T_e(Si, Sj, t_r)}{\partial g_L(t_1)} & \frac{\partial T_e(Si, Sj, t_r)}{\partial g_L(t_2)} & \frac{\partial T_e(Si, Sj, t_r)}{\partial g_L(t_3)} & \dots & \frac{\partial T_e(Si, Sj, t_r)}{\partial g_L(t_r)} \end{bmatrix}_{r \times r} \quad (30)$$

3.2 Objective Function for Steady-State Heat Conduction

For the steady-state case, the sensors are placed at the boundary Γ_2 . Therefore, the objective function is defined as

$$\min \left\{ \mathcal{J}_{g_L \text{ at } (x^\dagger, y^\dagger)} := \|\mathbf{T}_{\Gamma_2} - \mathbf{T}_m\|^2 : \text{Eq. (19) in } \Omega, \text{ BCs in Eqs. (20) and (21)} \right\} \quad (31)$$

where \mathbf{T}_m is the vector of the measured temperature. Eq. (31) can be expressed as

$$\mathcal{J} = \sum_{i=2}^{M-1} [T_{i,N} - T_{(i,N)_m}]^2 \quad (32)$$

where the $T_{i,N}$ and $T_{(i,N)_m}$, $i = 2, \dots, M-1$, are the estimated and measured temperatures at the outer surface Γ_2 , respectively. The gradient of the objective function \mathcal{J} with respect to the unknown heat source strength g_L is expressed as

$$\frac{\partial \mathcal{J}}{\partial g_L} = 2 \sum_{i=2}^{M-1} [T_{i,N} - T_{(i,N)_m}] \frac{\partial T_{i,N}}{\partial g_L} \quad (33)$$

Again, the sensitivity coefficients can be calculated using the chain rule as

$$\frac{\partial T_{i,N}}{\partial g_L} = \frac{\left(\frac{\partial T_{i,N}}{\partial k_T} \right)}{\left(\frac{\partial g_L}{\partial k_T} \Big|_{\text{at source place } L} \right)} \quad (34)$$

The term $\frac{\partial T_{i,N}}{\partial k_T}$ can be obtained from the boundary condition at the surface Γ_2 , Eq. (12). By solving the boundary condition equation for $T_{i,N}$ and then taking derivative of $T_{i,N}$ with respect to k_T , we obtain

$$\frac{\partial T_{i,N}}{\partial k_T} = - \frac{2h_2J\sqrt{\gamma}(-4\gamma T_{i,N-1} + \gamma T_{i,N-2} - \beta T_{i+1,N} + \beta T_{i-1,N} + 3\gamma T_{\infty_2})}{(3k_T\gamma + 2h_2J\sqrt{\gamma})^2} \quad (35)$$

The term $\frac{\partial g_L}{\partial k_T}$ is the same as the term for the transient case. Thus from Eq. (28), we have

$$\frac{\partial g_L}{\partial k_T} = \frac{-(4) \left(\alpha \frac{\partial^2 T_{Li,Lj}}{\partial \xi^2} - 2\beta \frac{\partial^2 T_{Li,Lj}}{\partial \xi \partial \eta} + \gamma \frac{\partial^2 T_{Li,Lj}}{\partial \eta^2} \right)}{J^2 n^2} \quad (36)$$

Thus the sensitivity coefficients for the steady-state heat conduction case will be as

$$\begin{aligned} \frac{\partial T_{i,N}}{\partial g_L} &= - \frac{(J^2 n^2) 2h_2 J \sqrt{\gamma} (-4\gamma T_{i,N-1} + \gamma T_{i,N-2} - \beta T_{i+1,N} + \beta T_{i-1,N} + 3\gamma T_{\infty_2})}{(-4) \left(\alpha \frac{\partial^2 T_{Li,Lj}}{\partial \xi^2} - 2\beta \frac{\partial^2 T_{Li,Lj}}{\partial \xi \partial \eta} + \gamma \frac{\partial^2 T_{Li,Lj}}{\partial \eta^2} \right) (3k_T \gamma + 2h_2 J \sqrt{\gamma})^2} = \\ &= \frac{J^3 n^2 h_2 \sqrt{\gamma} (-4\gamma T_{i,N-1} + \gamma T_{i,N-2} - \beta T_{i+1,N} + \beta T_{i-1,N} + 3\gamma T_{\infty_2})}{(2) \left(\alpha \frac{\partial^2 T_{Li,Lj}}{\partial \xi^2} - 2\beta \frac{\partial^2 T_{Li,Lj}}{\partial \xi \partial \eta} + \gamma \frac{\partial^2 T_{Li,Lj}}{\partial \eta^2} \right) (3k_T \gamma + 2h_2 J \sqrt{\gamma})^2} \end{aligned} \quad (37)$$

Sensitivity Analysis for Steady-State Heat Conduction

In this case, the sensitivity matrix $\mathbf{J}\mathbf{a}$ can be explicitly written as

$$\mathbf{J}\mathbf{a}_{g_L} = \begin{bmatrix} \frac{\partial T_{2,N}}{\partial g_L} \\ \frac{\partial T_{3,N}}{\partial g_L} \\ \vdots \\ \frac{\partial T_{M-1,N}}{\partial g_L} \end{bmatrix}_{(M-2) \times 1} \quad (38)$$

3.3 Minimization: Steepest Descent Method

The steepest descent minimization method used in this study is expressed as

$$\mathbf{g}_L^{(k+1)} = \mathbf{g}_L^{(k)} + \beta^{(k)} \mathbf{d}^{(k)} \text{ (transient heat conduction)} \quad (39)$$

$$g_L^{(k+1)} = g_L^{(k)} + \beta^{(k)} d^{(k)} \text{ (steady-state heat conduction)} \quad (40)$$

where $\mathbf{d}^{(k)}$ (and $d^{(k)}$) is the direction of steepest descent and $\beta^{(k)}$ is the search step size. The negative of the gradient direction $-\nabla \mathcal{J}^{(k)}$ denotes the direction of steepest descent $\mathbf{d}^{(k)}$. Thus,

$$\mathbf{d}^{(k)} = -\nabla \mathcal{J}^{(k)} \text{ (transient heat conduction)} \quad (41)$$

$$d^{(k)} = -\nabla \mathcal{J}^{(k)} \text{ (steady-state heat conduction)} \quad (42)$$

where the gradient direction $\nabla \mathcal{J}$ for the transient and steady-state heat conduction cases are defined in Eqs. (22) and (33), respectively. The search step size $\beta^{(k)} > 0$ is given by [1]

$$\beta^{(k)} = - \frac{\left[\mathbf{J}\mathbf{a}^{(k)} \mathbf{d}^{(k)} \right]^T [\mathbf{T}_e - \mathbf{T}_m]}{\left[\mathbf{J}\mathbf{a}^{(k)} \mathbf{d}^{(k)} \right]^T \left[\mathbf{J}\mathbf{a}^{(k)} \mathbf{d}^{(k)} \right]} \text{ (transient heat conduction)} \quad (43)$$

$$\beta^{(k)} = - \frac{[\mathbf{J}\mathbf{a}^{(k)} d^{(k)}]^T [\mathbf{T}_e - \mathbf{T}_m]}{[\mathbf{J}\mathbf{a}^{(k)} d^{(k)}]^T [\mathbf{J}\mathbf{a}^{(k)} d^{(k)}]} \quad (\text{steady-state heat conduction}) \quad (44)$$

Minimization Algorithm

The inverse analysis steps proposed in this study to estimate the constant and time-varying line heat source strengths can be summarized as below:

1. The temperature measurements are taken at the sensor place $S_{Si,Sj}$ and the time t_i ($i = 1, \dots, r$), $T_m(Si, Sj, t_i)$, for the transient case and the temperature measurements are taken at the outer surface Γ_2 , $T_{(i,N)_m}$, for the steady-state case.
2. The direct problem is solved to obtain the temperature values at the sensor place and the time t_i ($i = 1, \dots, r$), $T_e(Si, Sj, t_i)$, through solving Eq. (18) for the transient case and to obtain the temperature values at the outer surface Γ_2 , $T_{i,N}$, for the steady-state case. During the direct solution, the sensitivity coefficients (Eq. (23) for the transient case and Eq. (37) for the steady-state case) are computed. For the transient case, after the computations of the sensitivity coefficients (during the direct solution), the sensitivity matrix (Eq. (30)) can be computed as follows

```

doi = 1, r
do j = 1, r
  if (i.LT.j) then
    Ja(i, j) = 0.0
  else
    Ja(i, j) =  $\frac{T_{k_T}(i, 1)}{g_{L_{k_T}}(j, 1)}$ 
  endif
enddo
enddo

```

3. The objective function ($\mathcal{J}^{(k)}$) is computed using Eqs. (21) and (32) for the transient and steady-state cases, respectively.
4. The specified stopping criterion is examined for stopping or continuation of the minimization process.
5. The gradient direction $\nabla \mathcal{J}^{(k)}$, the direction of descent $\mathbf{d}^{(k)}$ (and $d^{(k)}$), and the search step size $\beta^{(k)}$ are computed.
6. \mathbf{g}_L (transient case) and g_L (steady-state case) are updated from Eqs. (39) and (40), respectively. Set the next iteration ($k = k + 1$) and return to the step 2.

3.4 Stopping Criterion

The minimization process to estimate the unknown variables can be stopped when the objective function is minimized sufficiently and stable and satisfactory results are obtained. In this study the minimization process is terminated when the objective function value $\mathcal{J}^{(k)}$ becomes less than a very small number ($\varepsilon = 10^{-5}$ or $\varepsilon = 10^{-6}$ depending on the test case). For the case of the temperature measurements with errors, the discrepancy principle is used. In the discrepancy principle, the minimization process can be stopped

when the difference between the estimated and measured temperatures is of the order of magnitude of the measurement errors. This can be mathematically expressed by

$$|T_e - T_m| \approx \sigma \quad (45)$$

where σ is the standard deviation of the measurement errors and is assumed constant. The stopping criteria can then be obtained by substituting Eq. (45) into the objective function expression for each of the transient (Eq. (21)) and steady-state (Eq. (32)) case, as follows

$$\varepsilon_{\text{transient}} = r\sigma^2 \quad (46)$$

$$\varepsilon_{\text{steady-state}} = (M - 2)\sigma^2 \quad (47)$$

The measured temperatures containing random errors T_{meas} are generated by adding an error term $\omega\sigma$ to the exact temperatures T_{exact} to give

$$T_{\text{meas}} = T_{\text{exact}} + \omega\sigma \quad (48)$$

where ω is a random variable with normal (Gaussian) distribution, zero mean, and unitary standard deviation. Assuming 99% confidence for the measured temperature, ω lies in the range $-2.576 \leq \omega \leq 2.576$ and it is randomly generated by using MATLAB.

4 Results

For each of the inverse transient and steady-state heat conduction problems, two test cases are presented. The data used in the test cases are so that they can reflect the accuracy, efficiency, and robustness of the proposed inverse analysis. At each test case, initially the direct heat conduction problem is solved with prescribed values of the line heat source strength to compute the temperature value at the sensor place. Then the computed temperatures are used as simulated measured ones to recover the prescribed values of the line heat source strength. For the function estimation problems (transient case), two different forms of timewise variation for the heat source are considered.

Before proceeding further, the steady-state and transient heat conduction equations are validated with the results from the commercial finite element software COMSOL. We assume that the heat conducting body is made of stainless steel (type 304) and the data used in the transient and steady-state test cases are listed in Tables 1 and 2, respectively. It should be added that all computations in this study are carried out using a Fortran compiler.

Table 1: Data used for the transient heat conduction problem (the body is made of stainless steel (type 304))

$\dot{q} \left(\frac{\text{W}}{\text{m}^2} \right)$	80000
$k_T \left(\frac{\text{W}}{\text{m} \cdot ^\circ\text{C}} \right)$	14.9
$\rho \left(\frac{\text{kg}}{\text{m}^3} \right)$	7900
$c \left(\frac{\text{J}}{\text{kg} \cdot ^\circ\text{C}} \right)$	477

(Continued)

Table 1 (continued)

$h_i \left(\frac{\text{W}}{\text{m}^2 \cdot ^\circ\text{C}} \right), i = 2, 3, 4$	6
$T_{\infty_i} (^\circ\text{C}), i = 2, 3, 4$	30
$g_L \left(\frac{\text{W}}{\text{m}} \right)$	$22000 + 2000 \sin \left(\frac{\pi t}{120} \right)$
$T_0 (^\circ\text{C})$	20
(Li, Lj)	(120, 120)
$(x^\dagger, y^\dagger) (\text{m})$	(0.220256331740, 0.291714547854)
$n (\text{in } \delta_n)$	80
mesh size $(M \times N)$	160×160
$t_r (\text{s}), \Delta t (\text{s})$	2000, 0.05

Table 2: Data used for the steady-state heat conduction problem (the body is made of stainless steel (type 304))

$\dot{q} \left(\frac{\text{W}}{\text{m}^2} \right)$	100
$k_T \left(\frac{\text{W}}{\text{m} \cdot ^\circ\text{C}} \right)$	14.9
$h_i \left(\frac{\text{W}}{\text{m}^2 \cdot ^\circ\text{C}} \right), i = 2, 3, 4$	6
$T_{\infty_i} (^\circ\text{C}), i = 2, 3, 4$	30
$g_L \left(\frac{\text{W}}{\text{m}} \right)$	500
(Li, Lj)	(60, 60)
$(x^\dagger, y^\dagger) (\text{m})$	(0.13504165411, 0.303559482098)
$n (\text{in } \delta_n)$	80
mesh size $(M \times N)$	90×90

The temperature distribution in the irregular heat conducting body for the transient heat transfer problem using the explicit code used in this study and the software COMSOL is shown in Fig. 2. Moreover, the temperature distribution along a radial line passing over the heat source computed by our code and COMSOL (Fig. 3) are compared (Fig. 4). And the temperature distribution in the irregular heat conducting body for the steady-state heat transfer problem using the explicit code and COMSOL is shown in Fig. 5. It can be seen that there is a good agreement between the results obtained from our code and the ones obtained from the software COMSOL confirming the accuracy of our code. Furthermore, the shape and the location of

the function $\delta_n(x - x^\dagger)\delta_n(y - y^\dagger) = \frac{n^2}{4 \cosh^2(n(x - x^\dagger)) \cosh^2(n(y - y^\dagger))}$ for $n = 80$ and $x^\dagger = 0.13504165411$ m and $y^\dagger = 0.303559482098$ m corresponding to the node $(Li, Lj) = (60, 60)$ (Table 2) is shown in Fig. 6. It can be seen that the maximum value of the function is at $x = x^\dagger$ and $y = y^\dagger$. Noting that in this study $n = 80$ and $\cosh^2(n(x - x^\dagger)) \cosh^2(n(y - y^\dagger))|_{(x=x^\dagger, y=y^\dagger)} = 1$, we obtain

$$\delta_{80}(x^\dagger - x^\dagger) \delta_{80}(y^\dagger - y^\dagger) = \frac{80^2}{4} = 1600 \quad (49)$$

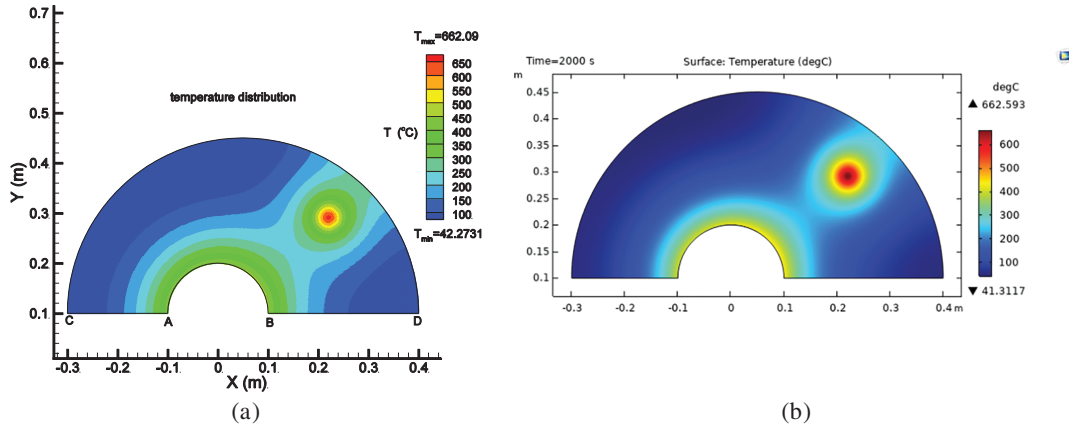


Figure 2: Validation of the transient heat conduction solver using the finite element software COMSOL. The result obtained by using our code (a) and the result obtained by using COMSOL (b)

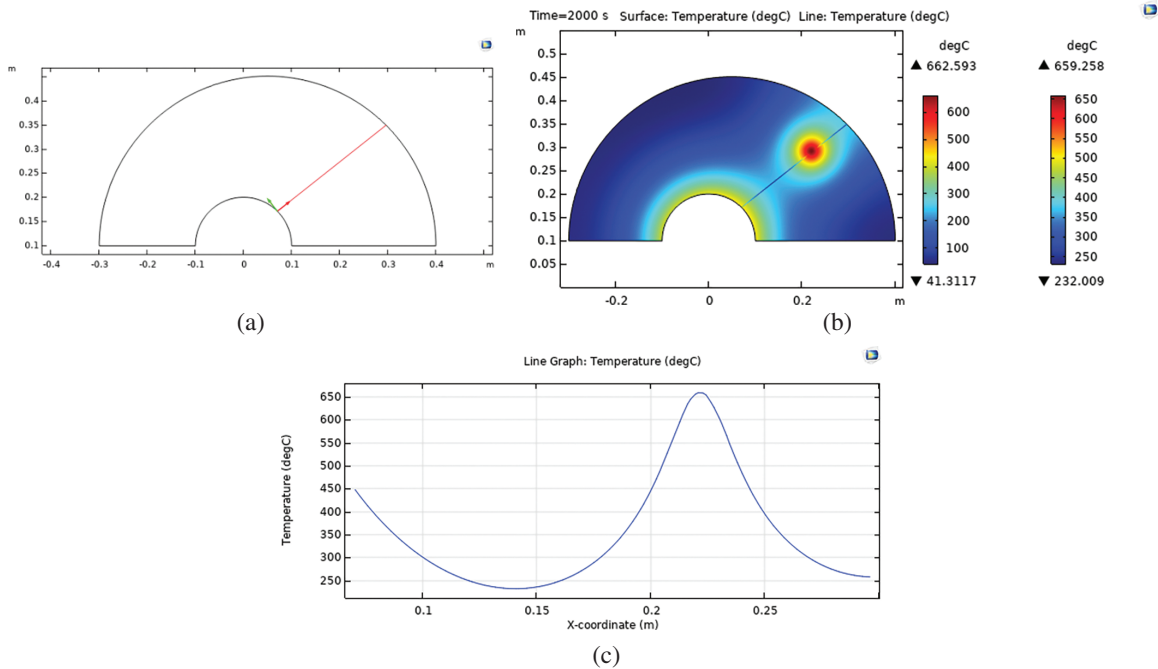


Figure 3: Temperature along a radial line passing over heat source obtained by software COMSOL. (a) the place of line (b,c) the temperature distribution

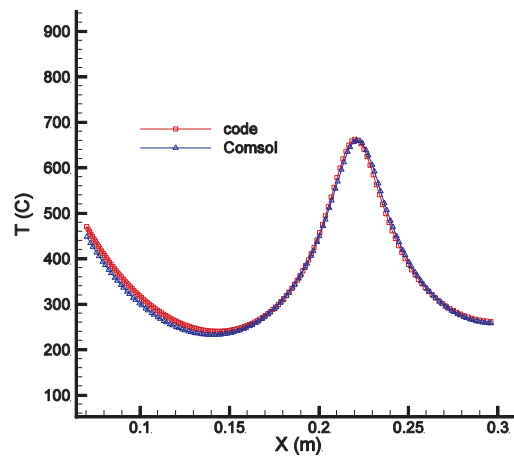


Figure 4: Comparison of temperature distribution along a radial line passing over heat source obtained by our code and software COMSOL

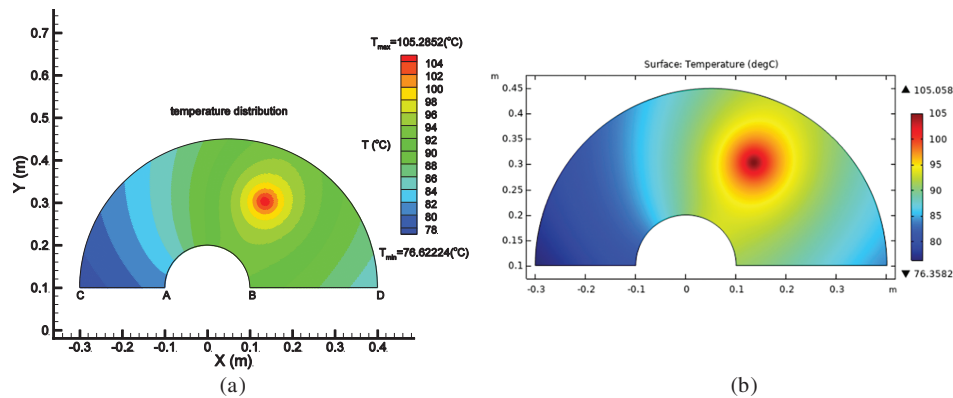


Figure 5: Validation of the steady-state heat conduction solver using the finite element software COMSOL. The result obtained by using our code (a) and the result obtained by using COMSOL (b)

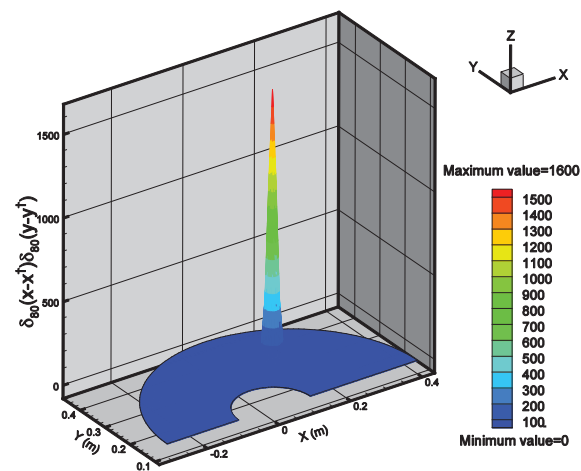


Figure 6: The shape and location of the function $\delta_n(x - x^\dagger) \delta_n(y - y^\dagger)$ for $n = 80$ and $x^\dagger = 0.13504165411$ m and $y^\dagger = 0.303559482098$ m

4.1 Test Cases 1 & 2 (Transient)

As mentioned previously, initially the direct transient heat conduction problem is solved using prescribed values of the line heat source strength ($g_L(t)_{\text{desired}}$) to compute the temperature value at the sensor place S_{S_i, S_j} and time t_i . Then the computed temperatures at the sensor place and time t_i are used as simulated measured ones to recover the prescribed values of the line heat source strength using an initial guess ($g_L(t)_{\text{initial}}$). The different forms of time wise variation for the heat source strengths for the transient test cases are given in Eqs. (50)–(53). And the data used in Test cases 1 & 2 are the same as the ones used for the validation test case (Table 1) except for the parameters listed in Table 3. The physical domain and the grid size (60×60) used for all four test cases are shown in Fig. 7. The estimation results for Test cases 1 & 2 including a comparison of the initial, final, and desired line heat source strengths (functions) as well as the objective function history are shown in Figs. 8 and 9, respectively. To investigate the effect of the measurement error on the inverse problem solution, two different measurement error levels are considered in the inverse analysis for Test case 1, including $\sigma = 0.01$ (Fig. 8c,d), and $\sigma = 0.1$ (Fig. 8e,f). It can be seen that the relatively good results are also obtained when there is large measurement error. In Test case 2, a more complicated initial guess is considered for the heat source strength to investigate the robustness of the proposed inverse analysis. As can be seen from the results for both test cases, there is an excellent agreement between the desired and final line heat source strengths, showing that the inverse analysis proposed in this study is very accurate and robust. As stated previously, all elements of the sensitivity matrix are computed during the heat equation solver without the need to solve the sensitivity and adjoint problems. So the computational cost for the inverse analysis at each iteration is approximately the same as the direct problem solution one. Despite the large number of the iterations in Test cases 1 & 2, the computation time is only a few hours on a PC with Intel Core i5 and 6G RAM.

$$g_L(t)_{\text{desired, Test case 1}} = 22000 + 2000 \sin\left(\frac{\pi t}{30}\right) \quad (50)$$

$$g_L(t)_{\text{initial, Test case 1}} = 22300 \quad (51)$$

$$g_L(t)_{\text{desired, Test case 2}} = \begin{cases} 18000, & 0 \leq t < 50s \\ \frac{21000 - 18000}{100 - 50} (t - 50) + 18000, & 50 \leq t < 100s \\ \frac{19000 - 21000}{150 - 100} (t - 100) + 21000, & 100 \leq t \leq 150s \\ 19000, & 150 < t \leq 200s \\ \frac{18000 - 19000}{250 - 200} (t - 200) + 19000, & 200 < t \leq 250s \\ 18000, & 250 < t \leq 300s \end{cases} \quad (52)$$

$$g_L(t)_{\text{initial, Test case 2}} = 18000 + 1000 \sin\left(\frac{\pi t}{60}\right) \quad (53)$$

Table 3: Data used for the transient heat conduction problem (Test cases 1 & 2)

	Test Case 1		Test Case 2	
$g_L \left(\frac{W}{m} \right)$	Desired:	Initial:	Desired:	Initial:
	$g_L(t)_{\text{desired, Test case 1}}$	$g_L(t)_{\text{initial, Test case 1}}$	$g_L(t)_{\text{desired, Test case 2}}$	$g_L(t)_{\text{initial, Test case 2}}$
(S_i, S_j) , sensor place	(40, 33)		(20, 30)	
	(0.109620697796 m, 0.273523509502 m)		(−0.0872990041971 m, 0.257627755404 m)	
(L_i, L_j) , source place	(40, 40)		(20, 40)	
(x^\dagger, y^\dagger) (m)	(0.130909919771, 0.301055127067)		(−0.102300945111, 0.294614402542)	
Mesh size $(M \times N)$	60×60		60×60	
t_r (s), Δt (s)	300, 0.2		300, 0.2	

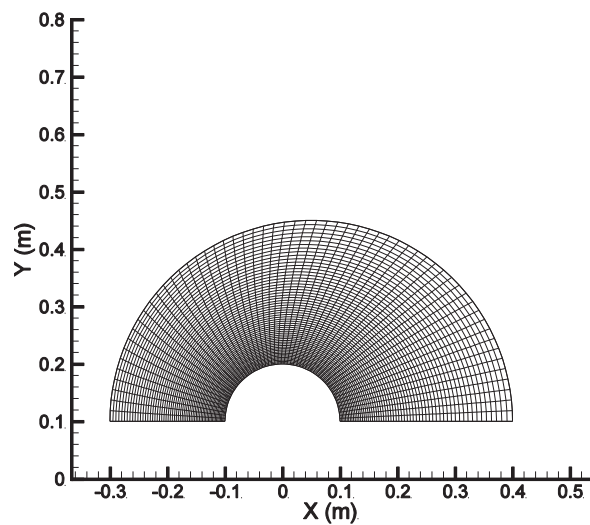


Figure 7: The physical domain and the grid size of 60×60 used for all test cases

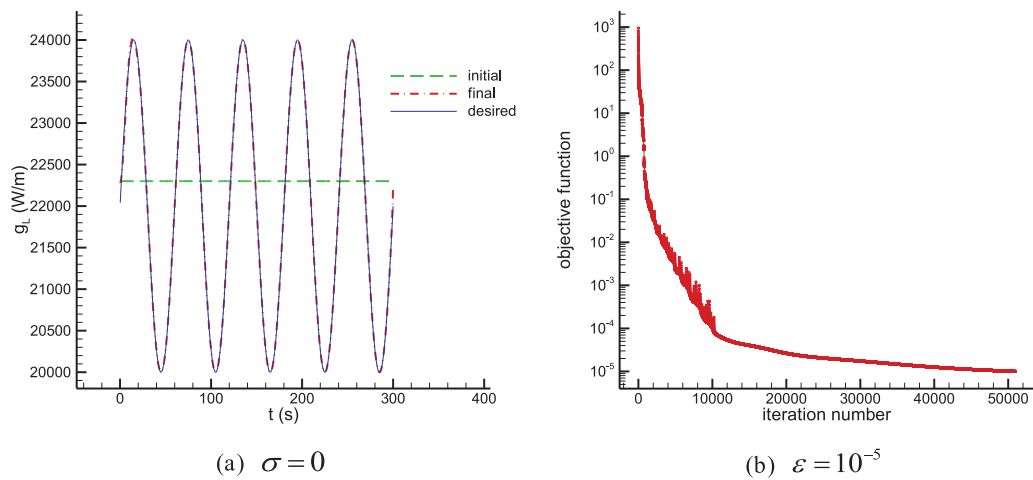


Figure 8: (Continued)

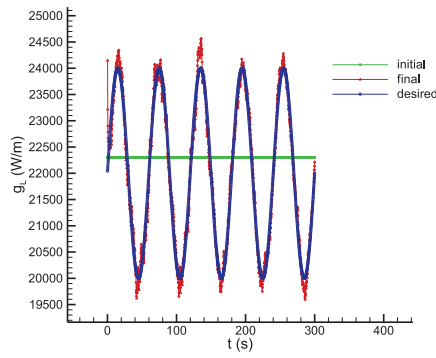
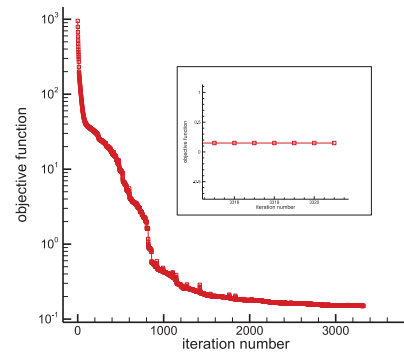
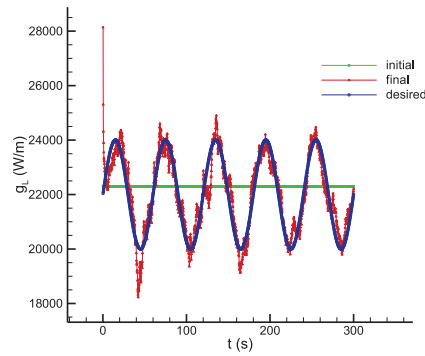
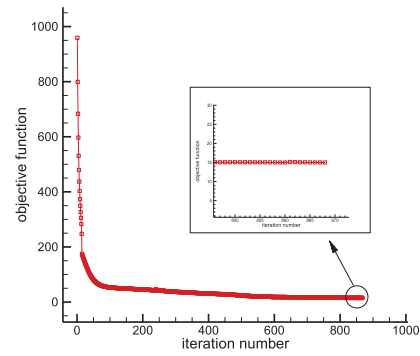
(c) $\sigma = 0.01$ (d) $\varepsilon = r\sigma^2 = \frac{t_r}{\Delta t}\sigma^2 = 0.15$ (e) $\sigma = 0.1$ (f) $\varepsilon = r\sigma^2 = \frac{t_r}{\Delta t}\sigma^2 = 15$

Figure 8: Test case 1 results. Estimation of the time-varying line heat source strength $g_L(t)$ using an initial guess $g_L(t)_{\text{initial, Test case 1}} = 22300 \left(\frac{\text{W}}{\text{m}}\right)$ and objective function versus iteration number for cases of no measurement error (a,b) and measurement errors of $\sigma = 0.01$ (c,d) and $\sigma = 0.1$ (e,f). The final time and time step are $t_r = 300$ (s) and $\Delta t = 0.2$ (s), respectively

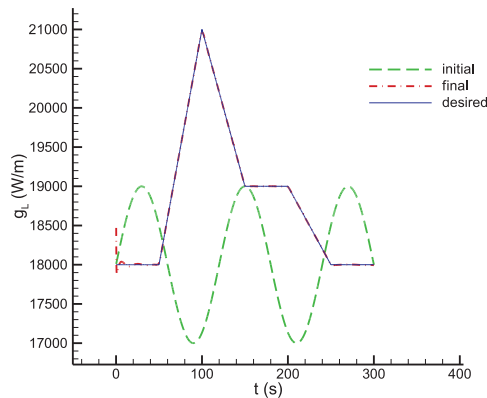
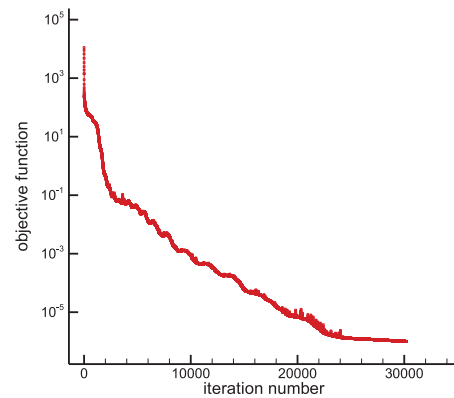
(a) $\sigma = 0$ (b) $\varepsilon = 10^{-6}$

Figure 9: Test case 2 results. Estimation of the time-varying line heat source strength $g_L(t)$ using an initial guess $g_L(t)_{\text{initial, Test case 2}} = \left(18000 + 1000 \sin\left(\frac{\pi t}{60}\right)\right) \left(\frac{\text{W}}{\text{m}}\right)$ and objective function versus iteration number for case of no measurement error (a,b)

From the results we can see that at the very early times t_i the estimated $g_L(t_i)$ deviate from the desired one because it takes time that the sensor be able to sense the variation in the temperatures caused by the heat source. Thus the sensitivity coefficients at the initial times are very small which shows that the large changes in $g_L(t_i)$ result in the small changes in $T_e(Si, Sj, t_i)$. In this case, the estimation of $g_L(t_i)$ becomes very difficult because the same value for $T_e(Si, Sj, t_i)$ would be obtained for a wide range of values of $g_L(t_i)$ [1]. Moreover, from the comparison shown in Fig. 8a we notice that in a neighborhood of t_r the estimated heat source deviates from the exact one and approaches the initially guessed value of the heat source. This can be due to this fact that by approaching the final time t_r , the number of the zero elements in the column vectors of the sensitivity matrix \mathbf{J}_a is gradually increased so that there exists only one nonzero element in the last column vector since the sensitivity matrix is a lower-triangular one. Therefore, the last column vector can be expressed as

$$\begin{bmatrix} 0 \\ 0 \\ 0 \\ \vdots \\ 0 \\ \frac{\partial T_e(Si, Sj, t_r)}{\partial g_L(t_r)} \end{bmatrix} \quad (54)$$

From Eq. (22), $\left(\frac{\partial \mathcal{J}}{\partial \mathbf{g}_L} = 2\mathbf{J}_a^T [\mathbf{T}_e - \mathbf{T}_m]\right)$, we can write the gradient of the objective function \mathcal{J} with respect to \mathbf{g}_L at the final time t_r as

$$\frac{\partial \mathcal{J}}{\partial g_L(t_r)} = 2 \begin{bmatrix} 0 \\ 0 \\ 0 \\ \vdots \\ 0 \\ \frac{\partial T_e(Si, Sj, t_r)}{\partial g_L(t_r)} \end{bmatrix}^T \begin{bmatrix} T_e(Si, Sj, t_1) - T_m(Si, Sj, t_1) \\ T_e(Si, Sj, t_2) - T_m(Si, Sj, t_2) \\ T_e(Si, Sj, t_3) - T_m(Si, Sj, t_3) \\ \vdots \\ T_e(Si, Sj, t_{r-1}) - T_m(Si, Sj, t_{r-1}) \\ T_e(Si, Sj, t_r) - T_m(Si, Sj, t_r) \end{bmatrix} = 2 \frac{\partial T_e(Si, Sj, t_r)}{\partial g_L(t_r)} [T_e(Si, Sj, t_r) - T_m(Si, Sj, t_r)] \quad (55)$$

which is a very small number. Substituting a very small value for $\nabla \mathcal{J}_{g_L(t_r)}^{(k)}$ into Eq. (41), $d_{g_L(t_r)}^{(k)} = -\nabla \mathcal{J}_{g_L(t_r)}^{(k)}$, results in a very small value for $d_{g_L(t_r)}^{(k)}$. Likewise, substituting a very small number for $d_{g_L(t_r)}^{(k)}$ into Eq. (39), $g_L(t_r)^{(k+1)} = g_L(t_r)^{(k)} + \beta^{(k)} d_{g_L(t_r)}^{(k)}$, results in $g_L(t_r)^{(k+1)} \approx g_L(t_r)^{(k)}$, as observed. In other words, by approaching the final time t_r , there is no significant modification in the value of g_L during the minimization process and the heat source retains its initially guessed value until the end of the minimization process.

Now in order to further investigate the effect of the initial guess on the minimization process and the estimated variable, a different initial guess is considered which is far from the desired heat source value. Once again Test case 2 is considered with the following constant line heat source strength as an initial guess:

$$g_L(t)_{\text{initial, Test case 2}} = 18500 \quad (56)$$

The result shown in Fig. 10 indicates the two points mentioned previously. Again, some deviations can be seen at very initial times as well as the final times. However, as it can be seen, the number of the deviated components of the estimated heat source is negligible compared to the total number of the components (which is $\frac{t_r}{\Delta t} = \frac{300}{0.2} = 1500$ in this test case).

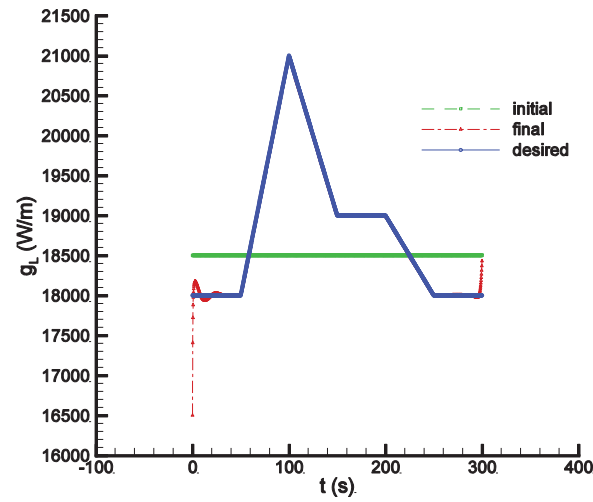


Figure 10: Test case 2 result. Estimation of the time-varying line heat source strength $g_L(t)$ using an initial guess $g_L(t)_{\text{initial, Test case 2}} = 18500 \left(\frac{\text{W}}{\text{m}} \right)$

4.2 Test Case 3 & 4 (Steady-State)

In Test cases 3 & 4, the objective is to recover the constant line heat source strength g_L using the simulated measurements and data given in Table 4. The convergence of the initial guess to the desired one and the objective function history is shown in Fig. 11 for Test case 3 and in Fig. 12 for Test case 4. In Test case 4, three different measurement errors of $\sigma = 0.1$, $\sigma = 1$, and $\sigma = 10$ are considered. Based on the maximum temperature at the boundary surface Γ_2 , these standard deviations represent 0.1%, 1%, and 10.6% temperature measurement error, respectively. The results shown in Table 5 show that the error in the recovered heat source strengths are 0.01%, 0.1%, and 1.17%, respectively. In other words, the error in the recovered variable is one tenth of the error in the temperature measurements which means that the proposed inverse analysis is not affected significantly by the measurement error. Moreover, the desired parameters are recovered within a few iterations with a little computational costs confirming the inverse analysis is very efficient.

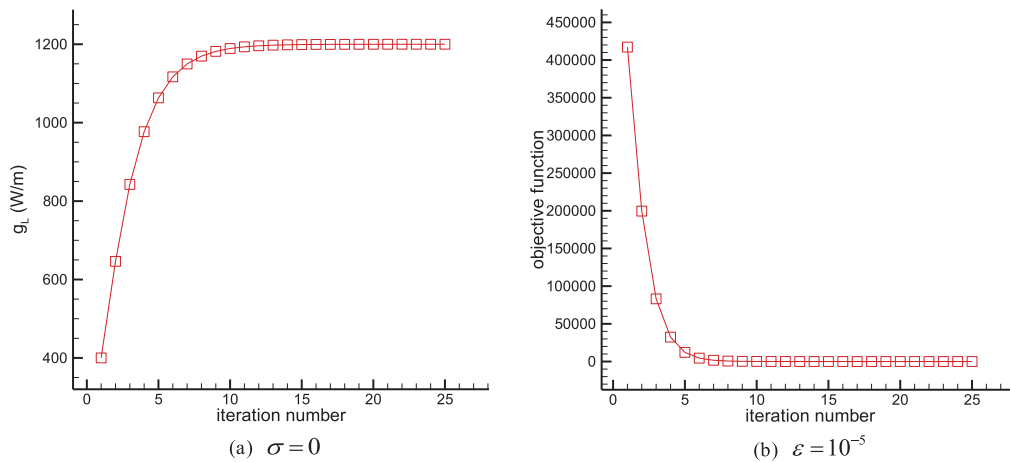


Figure 11: Test case 3 results. Estimation of the constant line heat source strength g_L using an initial guess $g_L_{\text{initial, Test case 3}} = 400 \left(\frac{\text{W}}{\text{m}} \right)$ and objective function vs. iteration number for case of no measurement error (a,b)

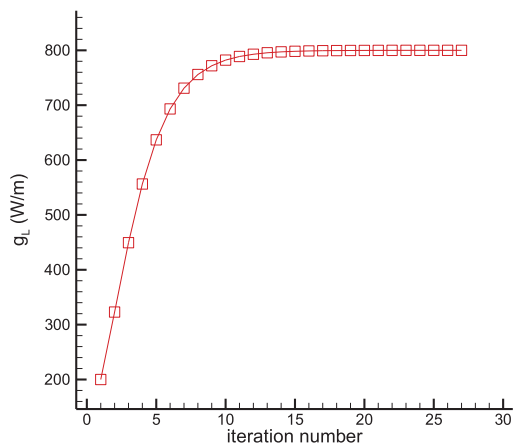
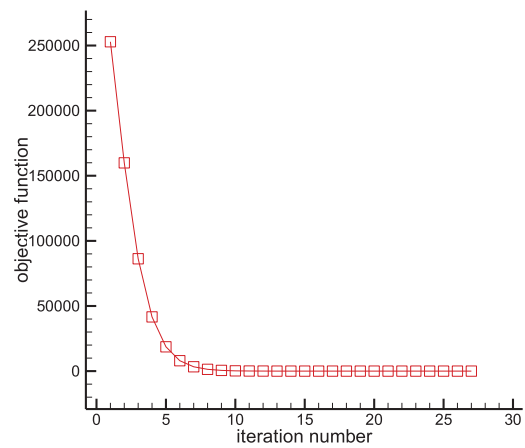
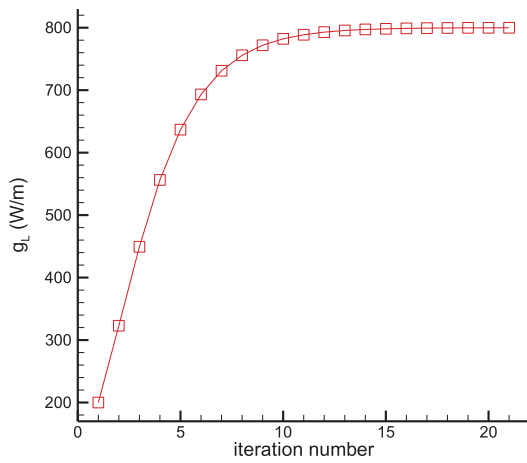
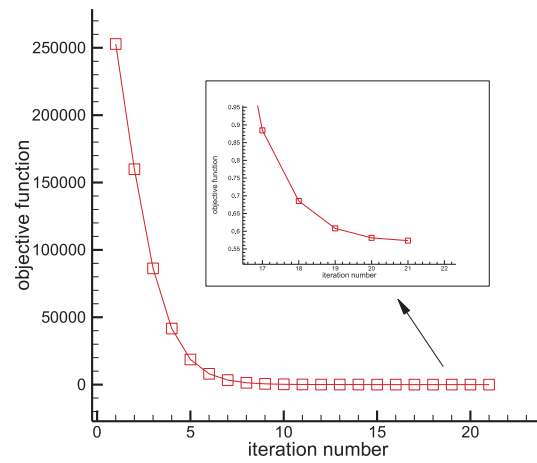
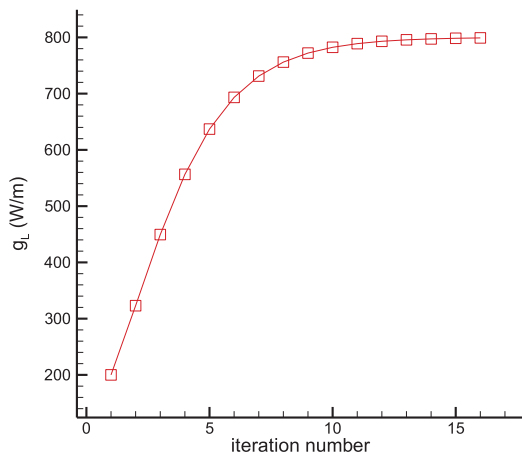
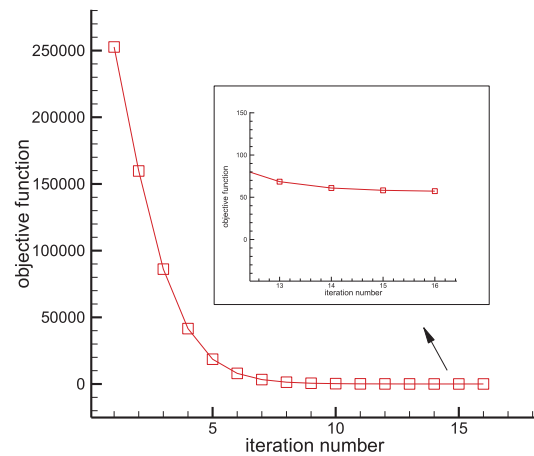
(a) $\sigma = 0$ (b) $\varepsilon = 10^{-5}$ (c) $\sigma = 0.1$ (d) $\varepsilon = (M-2)\sigma^2 = 58(0.1^2) = 0.58$ (e) $\sigma = 1$ (f) $\varepsilon = (M-2)\sigma^2 = 58(1^2) = 58$

Figure 12: (Continued)

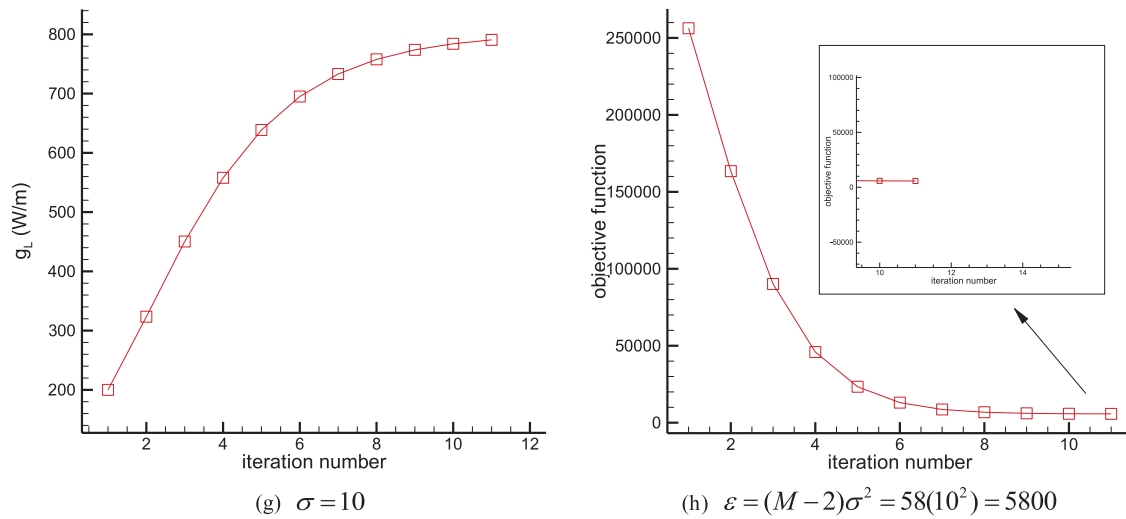


Figure 12: Test case 4 results. Estimation of the constant line heat source strength g_L using an initial guess $g_{L, \text{initial, Test case 4}} = 200 \left(\frac{\text{W}}{\text{m}} \right)$ and objective function vs. iteration number for case of no measurement error (a,b), and measurement errors of $\sigma = 0.1$ (c,d), $\sigma = 1$ (e,f), and $\sigma = 10$ (g,h)

Table 4: Data used for the steady-state heat conduction problem (the body is made of stainless steel (type 304))

	Test Case 3		Test Case 4	
$\dot{q} \left(\frac{\text{W}}{\text{m}^2} \right)$	700		900	
$k_T \left(\frac{\text{W}}{\text{m} \cdot ^\circ\text{C}} \right)$	14.9		14.9	
$h_i \left(\frac{\text{W}}{\text{m}^2 \cdot ^\circ\text{C}} \right), i = 2, 3, 4$	6		6	
$T_{\infty_i} (^\circ\text{C}), i = 2, 3, 4$	30		30	
$g_L \left(\frac{\text{W}}{\text{m}} \right)$	Desired: 1200	Initial: 400	Desired: 800	Initial: 200
(Li, Lj)	(40, 40)		(20, 20)	
$(x^\dagger, y^\dagger) (\text{m})$	(0.130909919739, 0.301055133343)		(-0.0738841593266, 0.227456390858)	
$n (\text{in } \delta_n)$	80		80	
mesh size $(M \times N)$	60×60		60×60	

Table 5: A summary of results for the estimation of constant line heat source strength in Test case 3 & 4

Test Case	Desired Value of g_L	Initial (Guess) Value of g_L	Final Value of g_L	Temperature Measurement Error, σ	Initial Value of \mathcal{J}	Final Value of \mathcal{J}
3	1200.00	400.00	1200.00	$\sigma = 0$	417,196.67	5.49×10^{-6}
4	800.00	200.00	800.00	$\sigma = 0$	252,857.20	2.58×10^{-6}
4	800.00	200.00	799.90 (error = 0.01%)	$\sigma = 0.1$	252,840.29	0.57

(Continued)

Table 5 (continued)

Test Case	Desired Value of g_L	Initial (Guess) Value of g_L	Final Value of g_L	Temperature Measurement Error, σ	Initial Value of \mathcal{J}	Final Value of \mathcal{J}
4	800.00	200.00	799.05 (error = 0.1%)	$\sigma = 1$	252,694.32	57.27
4	800.00	200.00	790.65 (error = 1.17%)	$\sigma = 10$	256,313.29	5726.26

Inverse crime. To avoid committing an inverse crime, a different mesh is also used to recover the desired heat source in Test case 4 with the largest measurement error of $\sigma = 10$. The simulated measurements are obtained using a mesh of size 60×60 (as in Test case 4). However, in the inverse analysis, a mesh of size 60×30 is used. Due to the mesh configuration, the heat source place is not exactly the same as the one used to generate the simulated measurements. Nevertheless, the results shown in Fig. 13 and Table 6 confirm that the proposed inverse analysis is accurate. The higher value obtained for the heat source can be due to the difference between the place of the heat source in two different mesh sizes. For the mesh of size 60×60 we have

$$(Li, Lj) = (20, 20)$$

$$(x^\dagger, y^\dagger) (\text{m}) = (-0.0738841593266, 0.227456390858)$$

and for the mesh of size 60×30 we have

$$(Li, Lj) = (20, 10)$$

$$(x^\dagger, y^\dagger) (\text{m}) = (-0.07273507582830, 0.224731139299)$$

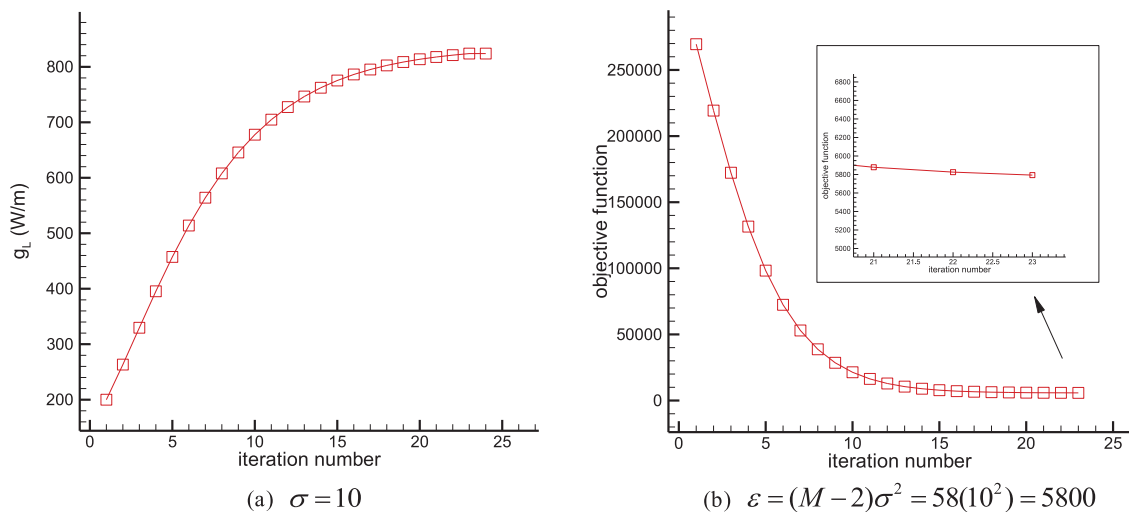


Figure 13: Test case 4 (different mesh size to avoid inverse crime) results. Estimation of the constant line heat source strength g_L using an initial guess $g_{L,\text{initial, Test case 4}} = 200 \left(\frac{\text{W}}{\text{m}} \right)$ and objective function versus iteration number for measurement error of $\sigma = 10$ (a,b)

Table 6: A summary of results for the estimation of constant line heat source strength in Test case 4 (different mesh size to avoid inverse crime)

Test Case	Desired Value of g_L	Initial (Guess) Value of g_L	Final Value of g_L	Temperature Measurement Error, σ	Initial Value of \mathcal{J}	Final Value of \mathcal{J}
4 (different mesh size to avoid inverse crime)	800.00	200.00	823.91 (error = 2.99%)	$\sigma = 10$	269,504.12	5793.18

5 Conclusion

This study presented an adjoint free gradient based inverse analysis to estimate a line heat source strength in the transient (function estimation) and steady-state (parameter estimation) inverse heat conduction problems over general 2D heat conducting bodies with the Neumann and Robin boundary conditions. Since the domain shape was irregular, a body-fitted grid generation method was used to mesh the domain. Then the heat conduction equations and the associated boundary conditions were transformed from the irregular physical domain to the regular computational domain to be able to use the finite difference method to discretize the equations. In the inverse analysis, an objective function is defined based on the least squares norm. Then using the chain rule and direct differentiation, an efficient, accurate, and very easy to implement sensitivity analysis was developed which enabled us to compute all the sensitivity coefficients during the direct heat transfer solution using the explicit expressions without the need to solve the sensitivity and adjoint problems to obtain the gradient of the objective function with respect to the unknown variables thereby reducing the computational cost of the inverse analysis significantly. The steepest descent method was used to minimize the objective function. By considering some levels of the measurement error, a few test cases were presented to reveal the accuracy of the method. The results from the test cases showed that the proposed inverse analysis is very accurate, efficient, and robust. In the steady-state cases, the analysis was not affected significantly by the measurement error. However, there was a relatively large error in the estimated function in the transient test cases when the measurement error was large as well.

Acknowledgement: Not applicable.

Funding Statement: The author received no specific funding for this study.

Availability of Data and Materials: The data that supports the findings of this study are available from the author upon reasonable request.

Ethics Approval: Not applicable.

Conflicts of Interest: The author declares no conflicts of interest to report regarding the present study.

References

1. Özışık MN, Orlande HR. Inverse heat transfer: fundamentals and applications. Oxfordshire, UK: Taylor & Francis; 2000.
2. Alifanov OM. Inverse heat transfer problems. Berlin/Heidelberg, Germany: Springer Science & Business Media; 2012.
3. Mohebbi F. Function estimation in inverse heat transfer problems based on parameter estimation approach. *Energies*. 2020;13(17):4410. doi:10.3390/en13174410.
4. Mohebbi F, Sellier M. Estimation of functional form of time-dependent heat transfer coefficient using an accurate and robust parameter estimation approach: an inverse analysis. *Energies*. 2021;14(16):5073. doi:10.3390/en14165073.

5. Lu ZR, Pan T, Wang L. A sparse regularization approach to inverse heat source identification. *Int J Heat Mass Transf.* 2019;142(12):118430. doi:10.1016/j.ijheatmasstransfer.2019.07.080.
6. Safari F, Duan Y. A novel meshless method in conjunction with a regularization technique for solving the transient heat source with additive noise. *Int Commun Heat Mass Transf.* 2024;158(25–26):107949. doi:10.1016/j.icheatmasstransfer.2024.107949.
7. Wei X, Huang A, Sun L. Singular boundary method for 2D and 3D heat source reconstruction. *Appl Math Lett.* 2020;102:106103. doi:10.1016/j.aml.2019.106103.
8. Lv C, Wang G, Chen H, Wan S. Estimation of the moving heat source intensity using the multiple model adaptive inverse method. *Int J Therm Sci.* 2019;138(3):576–85. doi:10.1016/j.ijthermalsci.2019.01.018.
9. Karkhin VA. *Thermal processes in welding.* Berlin/Heidelberg, Germany: Springer; 2019.
10. Silva Neto AJ, Özişik MN. Two-dimensional inverse heat conduction problem of estimating the time-varying strength of a line heat source. *J Appl Phys.* 1992;71(11):5357–62. doi:10.1063/1.350554.
11. Park HM, Chung OY, Lee JH. On the solution of inverse heat transfer problem using the Karhunen-Loève Galerkin method. *Int J Heat Mass Transf.* 1999;42(1):127–42. doi:10.1016/s0017-9310(98)00136-7.
12. Jarny Y. Determination of heat sources and heat transfer coefficient for two-dimensional heat flow—numerical and experimental study. *Int J Heat Mass Transf.* 2001;44(7):1309–22. doi:10.1016/s0017-9310(00)00186-1.
13. Liu FB. A modified genetic algorithm for solving the inverse heat transfer problem of estimating plan heat source. *Int J Heat Mass Transf.* 2008;51(15–16):3745–52. doi:10.1016/j.ijheatmasstransfer.2008.01.002.
14. Gu Y, Lei J, Fan CM, He XQ. The generalized finite difference method for an inverse time-dependent source problem associated with three-dimensional heat equation. *Eng Anal Bound Elem.* 2018;91(1):73–81. doi:10.1016/j.enganabound.2018.03.013.
15. Yan L, Fu CL, Yang FL. The method of fundamental solutions for the inverse heat source problem. *Eng Anal Bound Elem.* 2008;32(3):216–22. doi:10.1016/j.enganabound.2007.08.002.
16. Hazanee A, Lesnic D, Ismailov MI, Kerimov NB. An inverse time-dependent source problem for the heat equation with a non-classical boundary condition. *Appl Math Model.* 2015;39(20):6258–72. doi:10.1016/j.apm.2015.01.058.
17. Shah S, Parwani AK. Estimation of time-varying heat source for one-dimensional heat conduction by conjugate gradient method. In: *Innovations in infrastructure.* Singapore: Springer; 2018. p. 329–39. doi:10.1007/978-981-13-1966-2_29.
18. Lee KH. Application of repulsive particle swarm optimization for inverse heat conduction problem—parameter estimations of unknown plane heat source. *Int J Heat Mass Transf.* 2019;137:268–79. doi:10.1016/j.ijheatmasstransfer.2019.03.092.
19. Min T, Zang S, Chen S. Source strength identification problem for the three-dimensional inverse heat conduction equations. *Inverse Probl Sci Eng.* 2020;28(6):827–38. doi:10.1080/17415977.2019.1665663.
20. Necati OM. *Heat conduction.* Hoboken, NJ, USA: John Wiley & Sons; 1993.
21. Ozisik MN. *Finite difference methods in heat transfer.* Boca Raton, FL, USA: CRC Press; 1994.
22. Mohebbi F, Sellier M. Viscosity and effusion rate identification from free surface data. *Int J Thermofluids.* 2022;15:100184. doi:10.1016/j.ijft.2022.100184.